

Original paper

**Three-dimensional Fusion Images of Hepatic Vasculature and Bile Duct used for
Preoperative Simulation before Hepatic Surgery**

5 Atsushi Nanashima¹, Takafumi Abo¹, Ichiro Sakamoto², Hideyuki Hayashi², Toru Fukuda³,
Syuuichi Tobinaga¹, Masato Araki¹, Terumitsu Sawai¹, Takeshi Nagayasu¹,

¹ Division of Surgical Oncology and Department of Surgery, Nagasaki University Hospital,
1-7-1 Sakamoto, Nagasaki 8528501, Japan

10 ² Department of Radiology, Nagasaki University Hospital, 1-7-1 Sakamoto, Nagasaki
8528501, Japan

³ Section of Radiology, Nagasaki University Hospital, 1-7-1 Sakamoto, Nagasaki 8528501,
Japan

15 **Short title:** Preoperative simulation by 3D-fusion image

Correspondence: Atsushi Nanashima, M.D.,

Division of Surgical Oncology and Department of Surgery,

Nagasaki University Hospital, 1-7-1 Sakamoto, Nagasaki 852-8501, Japan

20 Tel: +81-95-819-7304, Fax: +81-95-819-7306

E-mail: a-nanasm@nagasaki-u.ac.jp

Abstract

Background/Aims: Recent developments in radiological technology allowed acquisition of
25 images with high spatial resolution that facilitate effective 3-dimensional (3D) reconstruction
of fusion images. Present study utilized 3D cholangiography and angiography with
multidetector-row computed tomography (MDCT) to acquire information regarding operative
simulations.

Methodology: 3D-fusion images were evaluated in 39 patients with hepatobiliary
30 malignancies who underwent surgical resections.

Results: An aberrant branch of segment 3 over the umbilical portal vein, a large hepatoma
compressed the hilar vessels, an aberrant branch of the caudate lobe vasculature in case of
metastatic liver tumor with a right-sided umbilical portal vein and transected biliary leakage
were clearly observed by 3D imaging system. Four patients with intrahepatic
35 cholangiocarcinoma underwent multiple biliary stent placement and adequate placement of
biliary stents was possible. In 22 patients with extrahepatic biliary carcinomas, visualization
of the extent of tumor invasion by 3D-fusion images was equivalent to conventional
cholangiography. In 2 patients, adequate placement of multiple stents could be visualized
with this system. In 2 patients who underwent hepatectomy, more extended cancer invasion
40 was observed than was visualized by 3D-fusion images.

Conclusions: 3D fusion images were very useful for preoperative simulations in order to
understand relationships between tumors and adjacent vasculatures.

Key words 3 dimensional, computed tomography, angiography, cholangiography, fusion
45 image

Abbreviations

3-dimensional (3D); multidetector-row computed tomography (MDCT); drip infusion
cholangiography (DIC); magnetic resonance image cholangiography (MRC); percutaneous
50 transhepatic cholangiography (PTC); endoscopic retrograde cholangiography (ERC); C-arm
with flat detector CT (C-arm CT)

INTRODUCTION

Imaging contributes to precise detection of tumor extent in hepatobiliary malignancies. Helical and multi-detector-row computed tomography (MDCT) and magnetic resonance image cholangiography (MRC) have been recently applied to diagnosis of hepatobiliary malignancies (1, 2). These imaging modalities can provide useful information regarding tumor infiltration and adjacent main hepatic vasculature. This information is necessary to have before surgery in order to achieve curative hepatectomy. With respect to cholangiography, however, direct cholangiography by percutaneous transhepatic cholangiography (PTC) and endoscopic retrograde cholangiography (ERC) is still a useful diagnostic tool for precise understanding of tumor infiltration, and its diagnostic accuracy is probably superior to that of MDCT and MRC at present (3, 4) However, conventional direct cholangiography has certain disadvantages, such as high exposure to radiation due to the need to take several views from various directions, administration of contrast media, and the long time that is required for examination. Furthermore, it is still difficult to compare angiographic and cholangiographic images and the resulting three-dimensional (3D) relationships of the vasculature.

3D imaging has been extensively applied in the field of radiology (4, 5). Contemporary MDCT and advanced workstation systems can provide accurate and clear 3D images of hepatic vasculature. Therefore, diagnostic accuracy has advanced remarkably (6, 7) Although drip-infusion cholangiography (DIC) is a classical method, very clear 3D-cholangiography can nowadays be obtained in patients without jaundice by MDCT (8) Furthermore, C-arm with flat detector CT (C-arm CT) has been recently developed for precise 3D-angiography, and can provide images with high spatial resolution with a single scan in short period of time (9, 10). An advantage of this system is that an immediate CT-like volume data set can be obtained without having to move the patient. Therefore, C-arm CT can be a practical clinical

tool that can deliver effective 3D information during interventional radiology. C-arm CT has been recently applied in various diseases including liver diseases (11, 12). The application and usefulness of C-arm CT in 7 patients with biliary malignancies was recently reported (13).

80 However, even with this new procedure it is still difficult to understand the spatial relationships between blood vessels and bile ducts. Therefore, it is necessary to obtain fusion images for each separate tumor image, as it is difficult to obtain CT-angiography and cholangiography simultaneously. To our knowledge, 3D-fusion imaging of angiography and cholangiography has not yet been extensively reported (11-14).

85 In the present study, 3D-fusion images between CT angiography and cholangiography were acquired with DIC-CT or C-arm CT in 39 patients with hepatobiliary malignancies who underwent surgical resection. The aim of this study was to apply this imaging procedure to preoperative simulation prior to hepatectomy.

90 METHODOLOGY

A total of 39 patients with hepatobiliary diseases who underwent surgical or radiological treatment at the Division of Surgical Oncology, Department of Surgery, Nagasaki University Hospital (NUH) between 2007 and 2010 were included. Patients included 26 males and 13 females, and their age ranged from 45 to 83 years (mean 69 ± 9 years). The diseases included
95 hepatocellular carcinoma (HCC) in 9, intrahepatic cholangiocarcinoma (ICC) in 5, metastatic colorectal carcinoma in 3, extrahepatic bile duct carcinoma in 17, and gall bladder carcinoma in 5 patients. Background liver diseases included normal liver in 15 patients, chronic hepatitis or cirrhosis in 8, and obstructive jaundice in 16 patients. Clinicopathological findings was according to the *Classification of Biliary Tract Carcinoma by Japanese Society of Biliary
100 Surgery (JSBS)*(15). The study design was approved by the Ethics Review Board of NUH and a signed consent form was obtained from each patient prior to participation in the study. Data was retrieved from patient charts in the NUH database for the duration of the initial hospitalization following hepatectomy.

Serial transverse scans with 0.5-mm thickness and 0.4-mm intervals were taken from
105 64-row multi-detector CT (AquilionTM 64; Toshiba Medical Systems Co., Tokyo, Japan) and the resulting images were stored. Using workstation software (Ziostation System 1000, version 1.31; Ziosoft Inc., Tokyo, Japan), actual areas without tumors and large vessels in the liver area were traced and measured. As contrast medium, either 100 ml of iopamidol (Oypalomin 370; Fuji-Pharma, Tokyo, Japan) for patients less than 60 kg or 135 ml of
110 iomeprol (Iomeron 350; Eizai, Tokyo, Japan) for patients over 60 kg was intravenously administrated via a bolus tracking-injection in an antecubital vein at a flow rate of 4 ml/s. The Hounsfield unit (HU) was set at 220 at the intraabdominal aorta. Under breath-hold, the arterial phase image was taken 5 s after injection, the portal phase image was taken at 20 s, and the hepatic venous phase was taken at 25 s. Each image acquisition took 7 s. Finally, the

115 equilibrium phase was taken at 150-180 s. Using workstation software (Ziostation System 1000, version 1.31; Ziosoft Inc., Tokyo, Japan), a radiological technician (T. F.) reconstructed 3D-CT angiography, as seen in Fig. 1A-C. Fusion images of the hepatic artery, portal vein and hepatic vein could be demonstrated by the workstation software (Fig. 1D).

For DIC-CT, 100 ml of iotroxic acid meglumine (Biliscopin DIC50; Bayer Healthcare, 120 Leverkusen, Germany) was intravenously administered. Patients underwent MDCT 30 min after injection. Using the same workstation software, 3D DIC-CT cholangiography was obtained, as is seen in Fig. 1E. Regarding direct cholangiography via PTC or an ERC drainage tube, 60% amido(dia-)trizoic acid (Urografin; Bayer Healthcare) diluted 10 times with saline was injected into the drainage tube. The C-arm CT and workstation system was 125 applied with the AXIOM Artis dBA and the syngo X-Workplace (Siemens Medical Solutions USA, Inc., Hoffman Estates, IL). This system is a cone beam CT with a flat detector (FD), and scanning was undertaken with rotation at an approximate angle of 200 degrees. CT-like reconstructed images were automatically constructed by the workstation. Scanning was performed once and lasted 8 s. Reconstruction of 3D images (in-space 3D) took 130 approximately 1 min after the scan completed. Output images were volume rendered in real-time images, maximum intensity projection (MIP) and multi-planer reconstruction (MPR) images. The obtained 3D cholangiographic images could be observed from any direction (Fig. 1F). Another option for exposing direct cholangiography, MDCT, was applied. During scanning the conventional MDCT, direct cholangiography was taken for 1 min was 135 taken between the hepatic venous phase and the equilibrium phase. The Hounsfield unit (HU) limit was set at 600.

RESULTS

The demographics of patients with intrahepatic malignant tumors with or without biliary infiltration who underwent preoperative 3D biliary and vascular imaging are shown in Table 1. All ICC located adjacent to the hilar bile duct and had involvements with bile duct. One HCC patient (Case 6) was preoperatively diagnosed with ICC with biliary involvement, which was a bile duct tumor thrombus by pathological findings. One metastatic liver carcinoma patient (Case 17) had invasion of a hilar bile duct and the portal vein. However, these invasions were not preoperatively diagnosed as biliary compression. The mean tumor size was 47 mm and ranged from 23-78 mm. Biliary stenosis or obstruction was observed in 11 patients (65%) and vascular invasion (almost to the portal vein) was observed in 8 patients. Preoperative biliary drainage was undertaken in only 6 patients with ICC diagnosed preoperatively. In 5 of these 6 patients, direct cholangiography applying FD-CT or MDCT and its fusion image with the hepatic vasculature was performed. Otherwise, the fusion image between DIC-CT and MDCT was reconstructed in order to diagnose the relationship between tumor location and the adjacent bile duct. A MIP image was taken in 6 patients in order to observe intraductal findings, for example with Cases 5, 7 and 16 (Figs. 2-4). Case 5 had ICC with hilar invasion (Fig. 2A) and direct 3D biliary imaging revealed an aberrant branch from the left hepatic duct to segment 3 over the umbilical portal vein (Fig. 2B) Case 7 had a large HCC located in the central liver which compressed the hilar bile duct and vasculature (Fig. 3A). To diagnose infiltration of HCC into the bile duct, the 3D-fusion image between DIC-CT and MDCT was taken (Fig. 3B), and neither bile duct tumor thrombus nor remarkable obstruction were observed. Therefore, biliary compression by the tumor was suspected preoperatively. In Case 16, metastatic liver carcinoma was located adjacent to hilar bile duct and portal trunk (Fig. 4A) and an extended right hepatectomy was scheduled. A right sided umbilical portal vein was confirmed with 3D-fusion vascular images (Fig. 4B).

Furthermore, the aberrant caudate lobe branched from the right hepatic duct (Fig. 4C). This caudate branch was not diagnosed preoperatively, and transected biliary leakage from the left remnant caudate lobe occurred after the right hepatectomy (Fig. 4D). An operation was undertaken in order to fix the leakage 8 months after the hepatectomy.

The post-treatment outcomes are shown in Table 2. Of the patients with ICC, 3 did not undergo surgical resection because of liver metastasis or peritoneal carcinomatosis, and 2 patients did not undergo surgical resection due to poor liver function. Four of 5 ICC patients underwent multiple biliary stent placement, and FD-CT was useful to adequately place metallic stents during frequent FD-CT cholangiography for interventional radiology (Case 2, Fig. 5). In Case 6, BDTT was observed during the operation. In Case 7, as diagnosed preoperatively, the compressed hilar bile duct was secured without biliary repair or anastomosis after hepatectomy for HCC. In Case 15, although the preoperative diagnosis was biliary compression (Fig. 6), the tumor was seen to have invaded the left bile duct during surgery. As described above, in Case 16, long-term biliary leakage occurred because of the failure in diagnosing the aberrant bile duct in segment 1.

The demographics of the 22 patients with extrahepatic carcinomas with biliary infiltration who underwent preoperative 3D biliary and vascular imaging are shown in Table 3. Biliary tract carcinomas were diagnosed with cholangiography and MDCT at our institute. Four patients had invasion of the portal vein (18%). Biliary drainage was performed in 19 patients (86%). Eleven patients (50%) had the fusion image with FD-CT cholangiography, 4 patients (18%) had the fusion image with MDCT accompanied with direct cholangiography, and 7 patients (32%) had the fusion image with DIC-CT and MDCT. Six of 12 patients with hilar bile duct carcinoma (HBDC) had cholangiography by MIP image, because MIP image was similar to two-dimensional (2D) cholangiography and easy to recognize the intraductal infiltration (Case 5, Fig. 1F-c). VR images also support diagnosis of hilar

cholangiocarcinoma (Fig. 7A, B). One HBDC patient without jaundice who had a DIC-CT image and a biliary stenosis in the right liver was clarified before operation although left
190 hepatectomy was resolved. (Case 6, Fig. 7C, D).

The post-treatment outcomes in patients with biliary tract carcinomas are shown in Table 4. Two HBDC patients did not undergo surgical resection due to poor liver function and liver metastasis. In those cases, FD-CT cholangiography was useful for placement of multiple stents in these patients (as well as for the ICC patients described above). In 2 patients,
195 extended cancer infiltration was observed with the intra-operative histological examination, which was not diagnosed by 3D or 2D cholangiography. One patient had superficial infiltration of the bile duct epithelium (Case 5) and another had extraductal perineural infiltration (Case 11). One patient had intraductal bleeding from the artery (A3), but otherwise had no related complications with biliary anastomoses.

200 **DISCUSSION**

Recent improvements in imaging technology have been remarkable. 3D imaging can be used for clinical diagnosis and provided useful information for surgical planning in various fields including hepatobiliary and pancreatic surgeries (16, 17). VR or MPR images from multi-detector row CT data allow for optimal display of vessels and adjacent organs by different degrees of opacity. The reconstructed 3D images can be viewed on a personal computer monitor. Hepatectomy for intrahepatic liver tumors or for extrahepatic biliary carcinomas is usually planned with preoperative imaging information regarding the relationship of the location of the tumor to the main hepatic vessels (such as the portal vein, hepatic artery, hepatic veins and hepatic ducts) (14, 18, 19). Preoperative simulation of hepatectomy by 3D imaging can be easier and more accurate than that by conventional axial imaging of CT or magnetic resonance imaging (MRI), due to the utility of viewing 3D images from any angle (20). At this stage, furthermore, scanning speeds of MDCT or C-arm CT were very fast, therefore the patient load was less in comparison with previous scanning techniques (21). The exposure of radiation was permitted in a safe limit for patient health. MRI also provides useful information for diagnosis of hepatobiliary malignancies (22). However, the spatial resolution of the activity is lower than of CT at our institute at this stage. In the case of combination with biliary information, fusion imaging may be difficult. Based on preoperative imaging information, understanding the anatomy was again confirmed by intraoperative ultrasound with the bubble contrast media (23, 24). In this way, the estimated hepatectomy was performed with more confidence. Preoperative 3D imaging information can be immediately confirmed with a personal computer during an operation, which can help to create a further sense of security and understanding.

220 Fusion between tumors and the biliary tract and vessels must be carefully reconstructed by the radiological technicians (RT) using a special workstation. In our institute,

225 a RT (T.F.) specially makes 3D-fusion images. Fusion images of the tumor and vascular
images might be easy to reconstruct, because all images can be obtained with the same
conditions and a small gap between the images, as is seen in Fig. 1a-c. However, consistency
of location between the biliary images and other images was difficult because of the time
difference between the image exposures. To solve this problem, direct imaging of the biliary
230 tract during MDCT exposure was simultaneously attempted, as described in the Methods
section. Moreover, the gap between the images could be minimized in the present pilot study.
With respect to cholangiography, C-arm CT and direct cholangiography during MDCT
provided accurate 3D images with a single scan within 10 s. Furthermore, with interventional
biliary stenting (as with Case 2), real-time 3D images can be obtained at each step of the
235 procedure. This makes this system a more powerful supporting system relative to
conventional 2D cholangiographic images (9-11, 13, 25). All MDCT, drip infusion CT and
MRCP provide excellent 3D cholangiographic images. However, biliary findings peripheral
to tumor stenosis is not often observed. C-arm CT provides various navigation data during
IVR, including various 3D images and CT-like images that include the surrounding tissue
240 (9-11, 13). The spatial resolution of 3D C-arm CT images is high. A previous report showed
that C-arm CT has been applied in liver diseases, and that small tumor lesions could be
observed by this modality (12, 26). Operation of the C-arm CT system is relatively
complicated, and the system is still relatively expensive.

In cases where the tumor was close to the main vessels (Cases 5, 7 and 15),
245 reconstruction of vessels or combined resection must be considered for radical resection (14).
In such cases, the distance and direction of tumor compression can be better estimated by
3D-fusion images than by single or 2D images (14, 16, 17, 25). If the spatial relationship
between a hepatic tumor and vessels is visualized, adequate hepatectomy could be easily
achieved and better surgical outcomes could result (27). In the case of a tumor closed or

250 compressed vessel, however, it is still difficult to define the real tumor involvement, even with 3D imaging at this point in time. More experience regarding 3D X-ray findings of tumor invasion is necessary by a prospective study in a larger number of patients to further this aim.

3D imaging is also useful to find pitfalls during operations. In Case 16 of the present study, atypical anatomy of the intrahepatic vessels was present which lead to a uncontrolled
255 bile leak. An aberrant bile duct in the caudate lobe of the liver was not detected, although upon further review the preoperative image clearly showed the anomaly. Right side umbilical portal vein is rare, and can include an atypical bile duct (28-31). Aberrant bile ducts in the caudate lobe are quite rare (32). When 3D cholangiography is diagnosed, it should be necessary to carefully observe such an aberrant vessels in the estimated remnant liver.

260 Furthermore, in Case 15, it was difficult to estimate what combined resection of bile duct was necessary, contrary to the HCC with Case 16. When a liver tumor is located adjacent to the hepatic hilum, the possibility of bile leakage after hepatectomy may not be rare (33). By considering the characteristics of tumor, and the differences between HCC and adenocarcinomas, reconstruction on the hilar vessels could be performed using 3D images
265 before the operation. In a case of hilar cholangiocarcinoma, the 3D-fusion images of hilar vessels provided useful information for understanding the relationship between the extent of tumor invasion in the bile duct and the guideposts of the vascular anatomy of portal vein and hepatic artery. In hepatectomy of hilar cholangiocarcinoma, the limit of the resection is usually decided by the umbilical portion or the confluence of the anterior and posterior
270 branch of the portal vein (34). Using 3D-fusion images, operative simulation can be performed by observing various views. In some cases without jaundice, 3D cholangiography by DIC-CT might be useful for detection of an obstructed bile duct (because static biliary tract could not be enhanced by this method). A case with decreasing liver function in the obstructed liver area by detected with ^{99m}-technetium galactosyl serum albumin (GSA) liver

275 scintigraphy was previously reported (35). Therefore, when such a case is observed, sectional dysfunction of the liver must be suspected.

Furthermore, in the present series, the different ways of performing 3D cholangiographic images such as VR, MIP or MPR were investigated (36). In comparison with VR images, it was easy to realize the extent of tumor invasion of hilar
280 cholangiocarcinoma by MIP images because MIP images resemble the conventional 2D images. In the present study, however, 3D images did not provide more useful information regarding diagnosing the extent of tumor invasion than by conventional 2D cholangiography. Moreover, in the present series, two cases showed more invasion in the bile duct wall (except for superficial extension) than preoperative diagnosis of 3D images (37). Further study to
285 examine the relationship between findings of 3D imaging and the real extent of hilar bile duct carcinomas is necessary in a larger number of subjects.

In conclusion, creation of 3D-fusion images from vascular images created by MDCT and cholangiography using FD-CT, simultaneous direct cholangiography, or DIC-CT is a newly developed tool that can provide useful information regarding the status of the extent of
290 tumor invasion and main vessels in the liver. Furthermore, examination time and radiation exposure are markedly reduced by the high speed and high resolution of the recently advanced CT imaging apparatus compared to standard 2D imaging. Therefore, preoperative simulation using this imaging modality can be potentially used on a large scale in order to provide supporting data in patients who undergo resection or other treatments, and may help
295 to improve curability and surgical safety.

REFERENCES

1. **Szklaruk J, Tamm E, Charnsangavej C:** Preoperative imaging of biliary tract
300 cancers. *Surg Oncol Clin N Am* 2002;11:865-876.
2. **Cho ES, Park MS, Yu JS, et al.:** Biliary ductal involvement of hilar
cholangiocarcinoma: multidetector computed tomography versus magnetic resonance
cholangiography. *J Comput Assist Tomogr* 2007;31:72-78.
3. **Otto G, Romanehsen B, Hoppe-Lotichius M, et al.:** Hilar cholangiocarcinoma:
305 resectability and radicality after routine diagnostic imaging. *J Hepatobiliary Pancreat
Surg* 2004;11:310-318.
4. **Vannier MW, Haller JW:** Navigation in diagnosis and therapy. *Eur J Radiol*
1999;31:132-140.
5. **Wiesent K, Barth K, Navab N, et al.:** Enhanced 3-D-reconstruction algorithm for
310 C-arm systems suitable for interventional procedures. *IEEE Trans Med Imaging*
2000;19:391-403.
6. **Kamel IR, Liapi E, Fishman EK:** Incidental nonneoplastic hypervascular lesions in
the noncirrhotic liver: diagnosis with 16-MDCT and 3D CT angiography. *Am J
Roentgenol* 2006;187:682-687.
7. **Uchida M, Ishibashi M, Tomita N, et al.:** Hilar and suprapancreatic
315 cholangiocarcinoma: value of 3D angiography and multiphase fusion images using
MDCT. *Am J Roentgenol* 2005;184:1572-1577.
8. **Persson A, Dahlström N, Smedby O, et al.:** Volume rendering of three-dimensional
drip infusion CT cholangiography in patients with suspected obstructive biliary disease:
320 a retrospective study. *Br J Radiol* 2005;78:1078-1085.

9. **Hirota S, Nakao N, Yamamoto S, et al.:** Cone-beam CT with flat-panel-detector digital angiography system: early experience in abdominal interventional procedures. *Cardiovasc Intervent Radiol* 2006;29:1034-1038.
10. **Meyer BC, Frericks BB, Albrecht T, et al.:** Contrast-enhanced abdominal
325 angiographic CT for intra-abdominal tumor embolization: a new tool for vessel and soft tissue visualization. *Cardiovasc Intervent Radiol* 2007;30:743-749.
11. **Orth RC, Wallace MJ, Kuo MD:** Technology Assessment Committee of the Society of Interventional Radiology. C-arm cone-beam CT: general principles and technical considerations for use in interventional radiology. *J Vasc Interv Radiol*
330 2008;19:814-820.
12. **Miyayama S, Matsui O, Yamashiro M, et al.:** Detection of hepatocellular carcinoma by CT during arterial portography using a cone-beam CT technology: comparison with conventional CTAP. *Abdom Imaging* 2009;34:502-506.
13. **Nanashima A, Abo T, Sakamoto I, et al.:** Three-dimensional cholangiography
335 applying C-arm computed tomography in bile duct carcinoma: a new radiological technique. *Hepatogastroenterology* 2009;56:615-618.
14. **Kamiyama T, Nakagawa T, Nakanishi K, et al.:** Preoperative evaluation of hepatic vasculature by three-dimensional computed tomography in patients undergoing hepatectomy. *World J Surg* 2006;30:400-409.
- 340 15. **Japanese Society of Biliary Surgery (JSBS).** Part I Anatomy In: Takukazu Nagakawa (ed) *Classification of Biliary Tract Carcinoma*. Second English ed., Kanehara & Co., LTD., Tokyo, p 2-10, 2004
16. **Fishman EK, Magid D, Ney DR, et al.:** Three-dimensional Imaging. *Radiology* 1991;181:321-337.

- 345 17. **Lee SW, Shinohara H, Matsuki M, et al.:** Preoperative simulation of vascular anatomy by three-dimensional computed tomography imaging in laparoscopic gastric cancer surgery. *J Am Coll Surg* 2003;197:927-936.
18. **Takahashi K, Sasaki R, Kondo T, et al.:** Preoperative 3D volumetric analysis for liver congestion applied in a patient with hilar cholangiocarcinoma. *Langenbecks Arch Surg* 2010;395:761-765.
- 350 19. **Numminen K, Sipilä O, Mäkisalo H:** *Eur J Radiol.* Preoperative hepatic 3D models: virtual liver resection using three-dimensional imaging technique 2005;56:179-184.
20. **Yamanaka J, Saito S, Fujimoto J:** Impact of preoperative planning using virtual segmental volumetry on liver resection for hepatocellular carcinoma. *World J Surg* 2007;31:1249-1255.
- 355 21. **Atasoy C, Akyar S:** Multidetector CT: contributions in liver imaging. *Eur J Radiol* 2004;52:2-17.
22. **Miller G, Schwartz LH, D'Angelica M:** The use of imaging in the diagnosis and staging of hepatobiliary malignancies. *Surg Oncol Clin N Am* 2007;16:343-368.
- 360 23. **Nakano H, Ishida Y, Hatakeyama T, et al.:** Contrast-enhanced intraoperative ultrasonography equipped with late Kupffer-phase image obtained by sonazoid in patients with colorectal liver metastases. *World J Gastroenterol* 2008;14:3207-3211.
24. **Nanashima A, Tobinaga S, Abo T, et al.:** Usefulness of sonazoid-ultrasonography during hepatectomy in patients with liver tumors: A preliminary study. *J Surg Oncol* 2011;103:152-157.
- 365 25. **Endo I, Shimada H, Sugita M, et al.:** Role of three-dimensional imaging in operative planning for hilar cholangiocarcinoma. *Surgery* 2007;142:666-675.

26. **Guckenberger M, Sweeney RA, Wilbert J, et al.:** Image-guided radiotherapy for liver cancer using respiratory-correlated computed tomography and cone-beam
370 computed tomography. *Int J Radiat Oncol Biol Phys* 2008;71:297-304.
27. **Liu JH, Chen PW, Asch SM, et al.:** Surgery for hepatocellular carcinoma: does it improve survival? *Ann Surg Oncol* 2004;11:298-303.
28. **Nagai M, Kubota K, Kawasaki S, et al.:** Are left-sided gallbladders really located on the left side? *Ann Surg* 1997;225:274-280.
- 375 29. **Kawai K, Koizumi M, Honma S, et al.:** Right ligamentum teres joining to the right branch of the portal vein. *Anat Sci Int* 2008;83:49-54.
30. **Si-Youn R, Poong-Man J:** Left-sided gallbladder with right-sided ligamentum teres hepatis: rare associated anomaly of exomphalos. *J Pediatr Surg* 2008;43:1390-1395.
31. **Hwang S, Lee SG, Park KM, et al.:** Hepatectomy of living donors with a left-sided
380 gallbladder and multiple combined anomalies for adult-to-adult living donor liver transplantation. *Liver Transpl* 2004;10:141-146.
32. **Munemasa Ryu:** Caudate lobe bile duct. In; Munemasa Ryu and Akihiro Cho (eds). *New Liver Anatomy. Portal Segmentation and the Drainage Vein.* Springer, NY, p75-80;2009
- 385 33. **Laurent A, Sauvanet A, Farges O, et al.:** Major hepatectomy for the treatment of complex bile duct injury. *Ann Surg* 2008;248:77-83.
34. **Hirano S, Tanaka E, Shichinohe T, et al.:** Treatment strategy for hilar cholangiocarcinoma, with special reference to the limits of ductal resection in right-sided hepatectomies. *J Hepatobiliary Pancreat Surg* 2007;14:429-433.
- 390 35. **Nanashima A, Sumida Y, Abo T, et al.:** Usefulness of measuring hepatic functional volume using Technetium-99m galactosyl serum albumin scintigraphy in bile duct carcinoma: report of two cases. *J Hepatobiliary Pancreat Surg* 2009;16:386-393.

395

36. **Saba L, Sanfilippo R, Montisci R, et al.:** Assessment of intracranial arterial stenosis with multidetector row CT angiography: a postprocessing techniques comparison. *Am J Neuroradiol* 2010;31:874-879
37. **Sakamoto E, Nimura Y, Hayakawa N, et al.:** The pattern of infiltration at the proximal border of hilar bile duct carcinoma: a histologic analysis of 62 resected cases. *Ann Surg* 1998;227:405-411.

400 **Figure legends**

FIGURE 1. 3D-CT angiography of the hepatic artery (A), portal vein (B) and hepatic vein (C) and their fusion images (D) demonstrated by workstation software. Cholangiography was obtained by DIC-CT (E), FD-CT (F) and direct cholangiography during MDCT.

405 VR image of FD-CT cholangiography shows stenosis of hilar bile duct by tumor infiltration.
a; Posterior view, stenotic right hepatic duct (arrow), stenotic left hepatic duct (dotted arrow).
b; Oblique view. c; MIP image of FD-CT cholangiography.

410 **FIGURE 2.** ICC with hilar and caval invasion in Case 5 (arrow) (A). Direct 3D biliary imaging shows the aberrant branch of segment 3 (dotted arrow) over the umbilical portal vein (UP) (solid line) (B).

FIGURE 3. A large HCC located in the central liver adjacent to the hepatic hilum,
415 and the 3D-fusion image using DIC-CT in Case 7. Oblique view (A). Caudal view (B).

FIGURE 4. Metastatic liver carcinoma located adjacent to hilar bile duct in Case 16
(A) and the 3D-fusion images with DIC-cholangiography showing right side umbilical
420 portal vein (arrow) (B). Bile duct of the left caudate lobe branched from the right hepatic duct (arrow) (C) and transected biliary leakage from the left remnant caudate lobe (arrowhead) (D).

425 **FIGURE 5.** Multiple biliary stents (arrow) placed while applying FD-CT
cholangiography during interventional radiology in Case 2.

FIGURE 6. Preoperative diagnosis was biliary compression (arrow) in Case 15. A
tumor (T) invaded the left hepatic duct (BD).

430

FIGURE 7. Hilar bile duct carcinoma (HBDC) invading the right and left biliary
tracts (arrow) in Case 5 (A), showing the portal vein (PV) and hepatic artery (HA).
Another HBDC patient without jaundice, Case 6, had a biliary obstruction in the right
liver (arrow) detected by DIC-CT cholangiography (C). Left hepatic duct (dotted
435 arrow) was drained by a plastic tube stent.

TABLE 1 Demographics of Patients with Intrahepatic Liver Tumors and 3D Vascular and Bile Duct Fusion Images.

	Diseases	Age (years) Gender	Tumor Size (mm)	Tumor Location	Biliary stenosis*	Vascular invasion	Biliary drainage	Cholangio graphy	3D image	Pretreatment diagnosis biliary invasion
1	ICC with HI	74 Male	56	Sg4	Brlc	PV	yes	D; FD-CT	VR	BI
2	ICC with HI	53 Male	78	Sg45	Brlc	PV	yes	D; FD-CT	VR	BI
3	ICC with HI	48 Male	34	Sg451	Brlc	PV	yes	D; FD-CT	VR	BI
4	ICC with HI	63 Male	41	Sg451	Brlc	PV	yes	D; FD-CT	VR, MIP	BI
5	ICC with HI	72 Male	36	Sg567	Brlc	PV, IVC	yes	D; CT	VR, MIP	BI, identify aberrant B3
6	HCC with BDTT	68 Male	23	Sg8	Br	PV	yes	I; DIC-CT	VR, MIP	BI
7	HCC	74 Female	54	Sg4	Brl		no	I; DIC-CT	VR, MIP	BC
8	HCC	78 Male	33	S67			no	I; DIC-CT	VR	none; identify B6
9	HCC	75 Male	35	S5			no	I; DIC-CT	VR	none; identify B58
10	HCC	73 Female	28	S78			no	I; DIC-CT	VR	none; identify B678
11	HCC	45 Male	28	S5			no	I; DIC-CT	VR	none; identify B58
12	HCC	66 Male	41	S56			no	I; DIC-CT	VR, MIP	none; identify B5678
13	HCC	84 Male	60	S567			no	I; DIC-CT	VR	BC
14	HCC	78 Male	75	S45678	Brl		no	I; DIC-CT	VR	BC
15	MLC	80 Female	34	S4	Bl		no	I; DIC-CT	VR	BC
16	MLC	67 Male	32	S48	Brlc	PV	no	I; DIC-CT	VR, MIP	BC, aberrant left B1
17	MLC with HI	70 Male	65	S234	Bl	PV	no	I; DIC-CT	VR	BC

440 ICC; intrahepatic cholangiocarcinoma, HI; hilar bile duct invasion, HCC; hepatocellular carcinoma, BDTT; bile duct tumor thrombosis, PV; portal vein, IVC; inferior vena cava, MLC; metastatic liver carcinoma, D; direct cholangiography, I; indirect cholangiography, CT; computed tomography; FD; flat-detector (Dyna), DIC; drip infusion cholangiography, VR; volume rendering image, MIP; maximum intensity projection image

445 * Findings of extend of biliary stenosis according to the Classification of Biliary Tract Carcinoma by Japanese Society of Biliary Surgery (JSBS)(15), Br; right hepatic bile duct, Bl; left hepatic bile duct, Bc; confluence of the right and left hepatic bile ducts, Bs; superior bile duct, Bm; middle bile duct, Bi; inferior bile duct. BI; biliary invasion, BC; biliary compression

TABLE 2 Operative Outcomes of Patients with Intrahepatic Liver Tumors with 3D Vascular and Bile Duct Fusion Images.

	Treatments	Differences from preoperative image	Post-treatment complications
1	Probe laparotomy	none	-
2	Multiple BS	none	-
3	Multiple BS	none	-
4	Multiple BS	none	-
5	Multiple BS	none	-
6	Right hepatectomy	BDTT	ascites
7	Central bisegmentectomy	none	nil
8	Segmentectomy (Sg6)	none	nil
9	Segmentectomy (Sg56)	none	nil
10	Segmentectomy (Sg78)	none	nil
11	Segmentectomy (Sg5)	none	nil
12	Right hepatectomy	none	nil
13	Right hepatectomy	none	nil
14	Right trisectionectomy	none	nil
15	Left hepatectomy	left BD invasion	nil
16	Right hepatectomy	none	long-term bile leak
17	Left hepatectomy	none	nil

BS; biliary stent placement, BDTT; bile duct tumor thrombosis

450 **TABLE 3** Demographics of Patients with Extrahepatic Biliary Tumors and 3D Vascular and Bile Duct Fusion Images.

	Diseases	Age (years) Gender	Tumor Size (mm)	Vascular invasion	Biliary stenosis*	Biliary drainage	Cholangiogra- phy	3D image	Pretreatment diagnosis biliary invasion
1	HBDC	76 Female	42	PV	Brlcs	yes	D; FD-CT	VR	BI
2	HBDC	68 Female	38		Brlc	yes	D; FD-CT	VR	BI
3	HBDC	70 Male	-	-	Brlc	yes	D; FD-CT	VR	BI
4	HBDC	82 Female	-	-	Brlcs	yes	D; FD-CT	VR, MIP	BI
5	HBDC	60 Male	56	no	Brlcsm	yes	D; FD-CT	VR, MIP	BI
6	HBDC	75 Female	43	no	Brlc	yes	I; DIC-CT	VR, MIP	BI
7	HBDC	60 Male	44	no	Brlcs	yes	D; FD-CT	VR, MIP	BI
8	HBDC	55 Female	33	no	Bl	yes	D; FD-CT	VR, MIP	BI
9	HBDC	83 Female	43	no	Brlcs	yes	I; DIC-CT	VR	BI
10	HBDC	72 Male	-	-	Brlcsm	yes	D; CT	VR	BI
11	HBDC	75 Male	48	PV	Brlcsmi	yes	D; CT	VR	BI
12	HBDC	72 Male	68	no	Brlcsm	yes	D; FD-CT	VR, MIP	BI
13	BDC	61 Female	-	-	Bsm	yes	I; DIC-CT	VR	BI
14	BDC	78 Male	35	no	Bsmi	yes	D; FD-CT	VR	BI
15	BDC	73 Male	34	no	Bsm	yes	D; FD-CT	VR	BI
16	BDC	64 Male	32	no	Bmi	no	D; FD-CT	VR	BI
17	BDC	77 Female	35	no	Bsmi	yes	I; DIC-CT	VR	BI
18	GBC	65 Male	27	no	Bsm	no	I; DIC-CT	VR	BI
19	GBC	66 Female	-	-	Brlcsm	yes	D; CT	VR	none
20	GBC	65 Female	78	PV	Br	no	I; DIC-CT	VR	BC
21	GBC	80 Male	66	PV	Brlcsm	yes	I; DIC-CT	VR	BI
22	GBC	69 Male	45	-	Brlcsmi	yes	D; CT	VR, MIP	BI

HBDC; hilar bile duct carcinoma, BDC; bile duct carcinoma, GBC; gallbladder carcinoma, D; direct cholangiography, I; indirect cholangiography, CT; computed tomography; FD; flat-detector (Dyna), DIC; drip infusion cholangiography, VR; volume rendering image, MIP; maximum intensity projection image

455 * Findings of extend of biliary stenosis according to Classification of Biliary Tract Carcinoma by Japanese Society of Biliary Surgery (JSBS)(15), Br; right hepatic bile duct, Bl; left hepatic bile duct, Bc; confluence of the right and left hepatic bile ducts, Bs; superior bile duct, Bm; middle bile duct, Bi; inferior bile duct. BI; biliary invasion, BC; biliary compression

Table 4 Operative Outcomes of Patients with Intrahepatic Liver Tumors with 3D Vascular and Bile Duct Fusion Images.

	Treatments	Differences from preoperative image	Post-treatment complications
1	Right trisectionectomy+BDR	none	wound infection
2	Left hepatectomy+BDR	none	nil
3	Multiple BS	-	-
4	Multiple BS	-	-
5	Left hepatectomy+BDR	infiltration to Bi	nil
6	Left hepatectomy+BDR	none	nil
7	Left hepatectomy+BDR	none	nil
8	Left hepatectomy+BDR	none	nil
9	Right hepatectomy+BDR+PVR	none	nil
10	BS	-	-
11	Right hepatectomy+PD	infiltration to B23	Intra-ductal bleeding of the bile duct stump, ascites
12	Right hepatectomy+PD	none	nil
13	BS	none	-
14	PD	none	pancreatic fistula
15	PD	none	pancreatic fistula
16	PD	none	nil
17	Segmentectomy 45 +BDR	none	-
18	BS	-	nil
19	Right trisectionectomy	none	-
20	BS	-	nil
21	BS	-	-
22	Right hepatectomy+PD+PVR	none	pancreatic fistula

BS; biliary stent placement, BDR; resection of bile duct, PVR; resection of portal vein, PD; pancreaticoduodenectomy

Fig 1

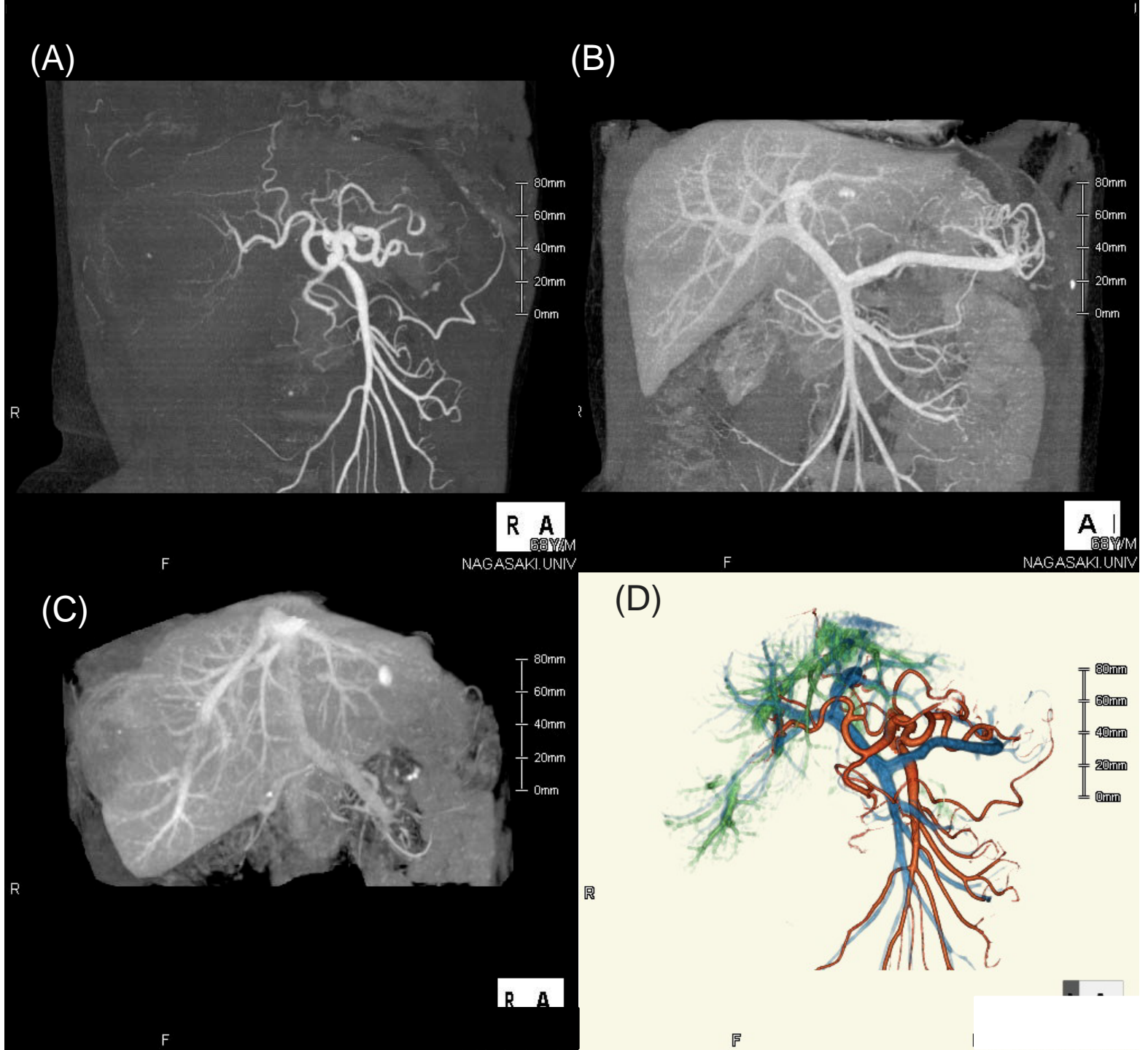


Fig 1E-F

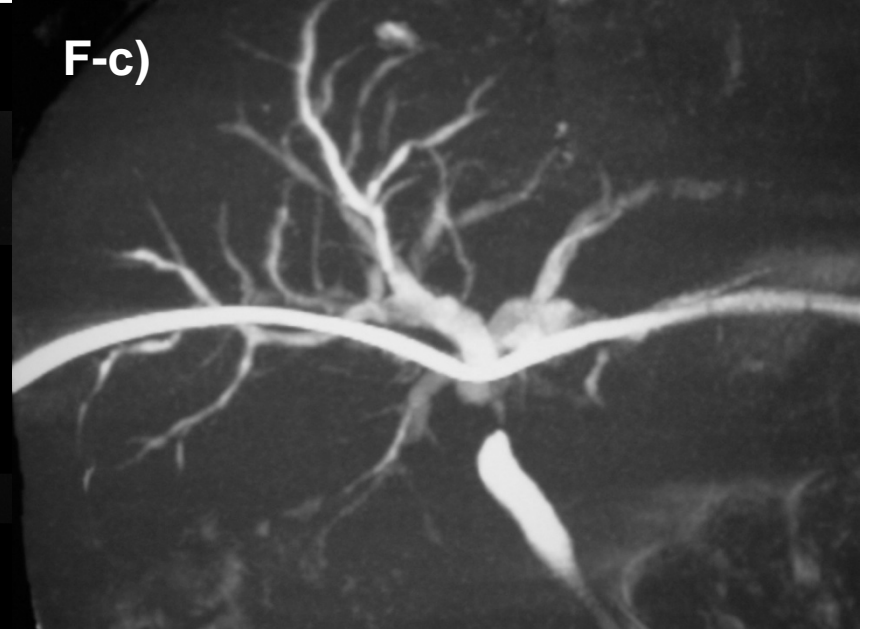
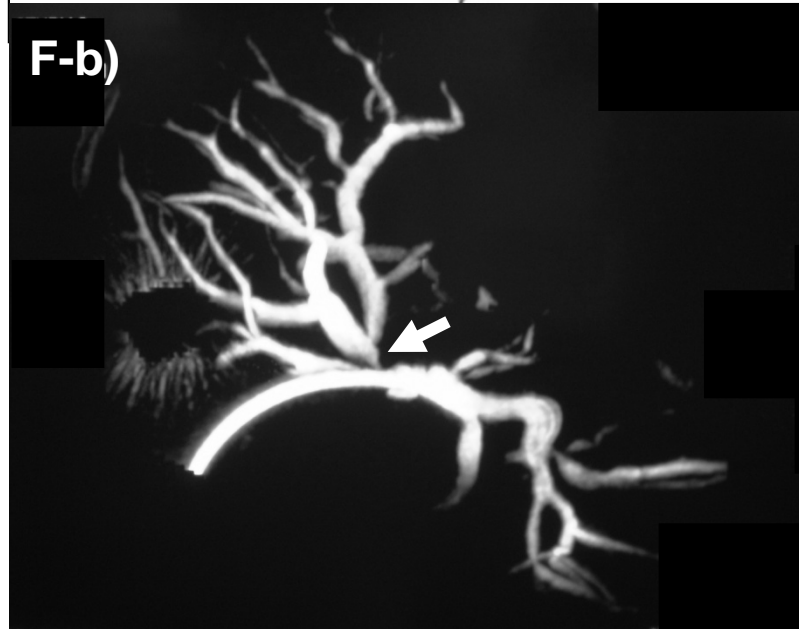
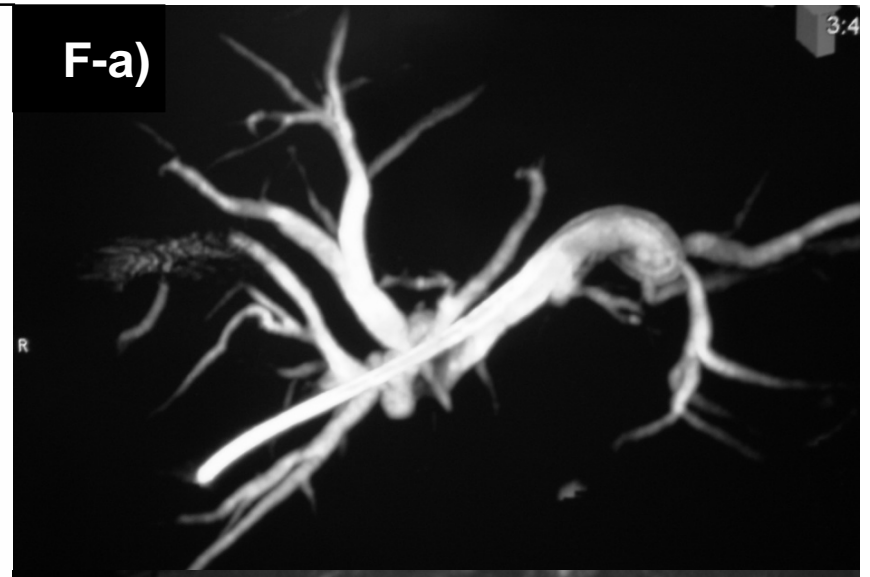
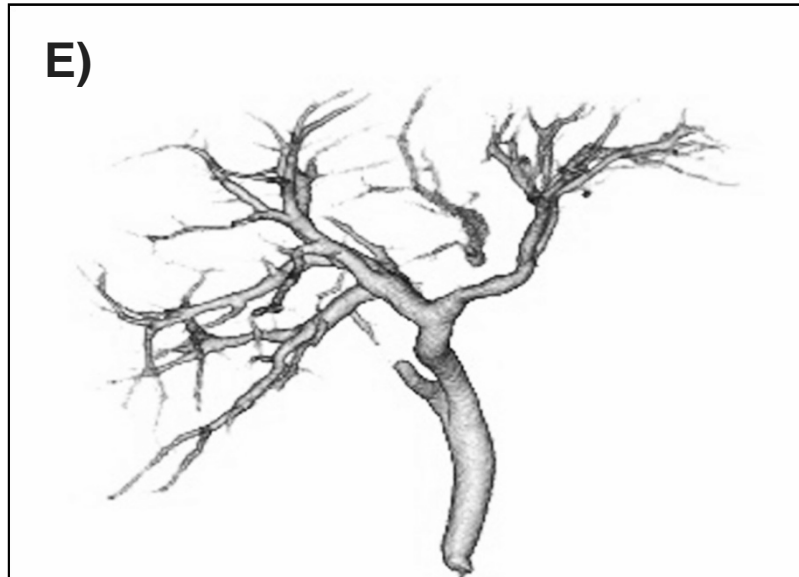
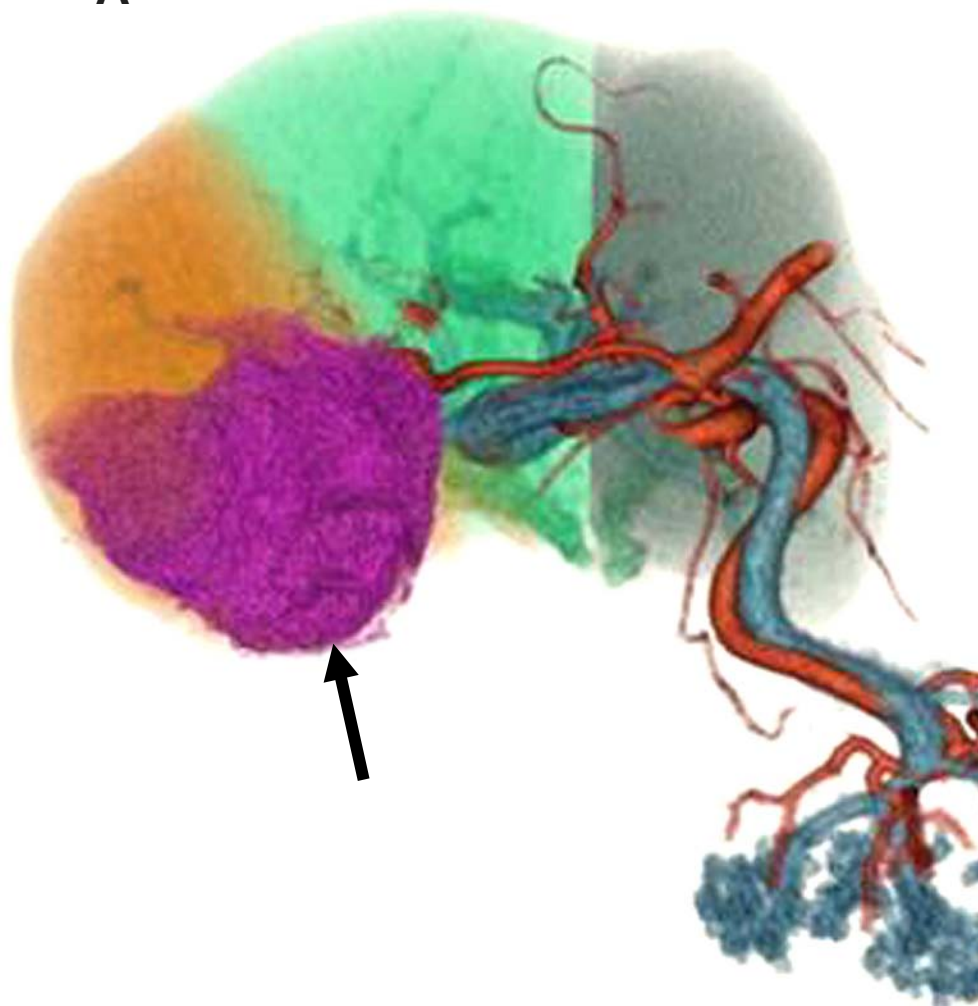


Fig 2

A



B

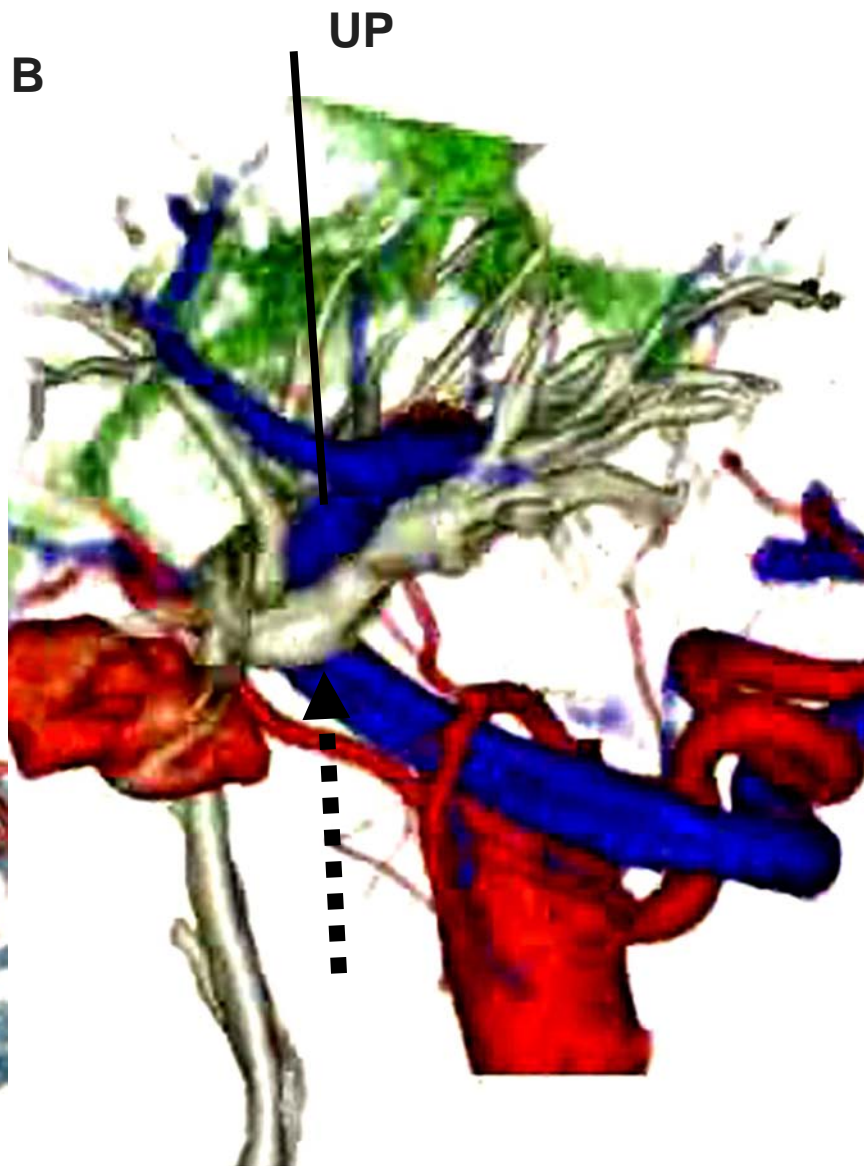
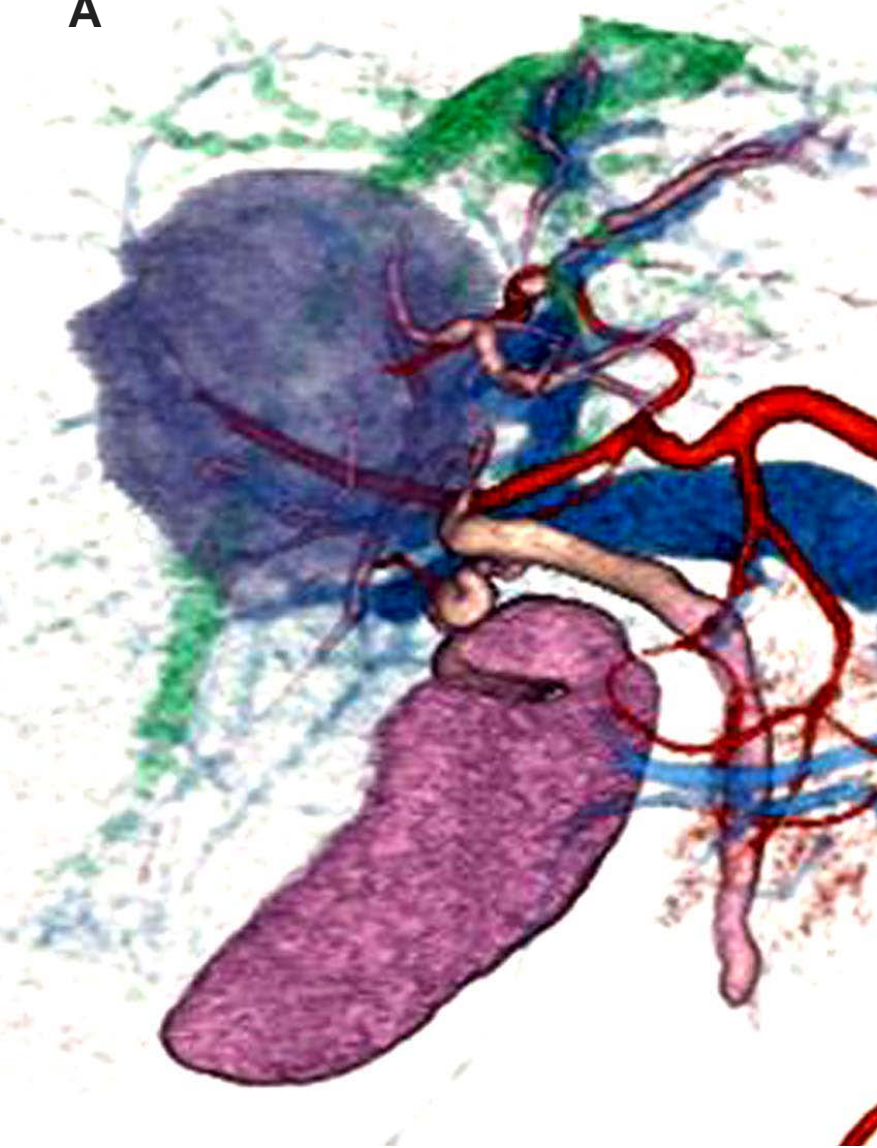


Fig 3

A



B

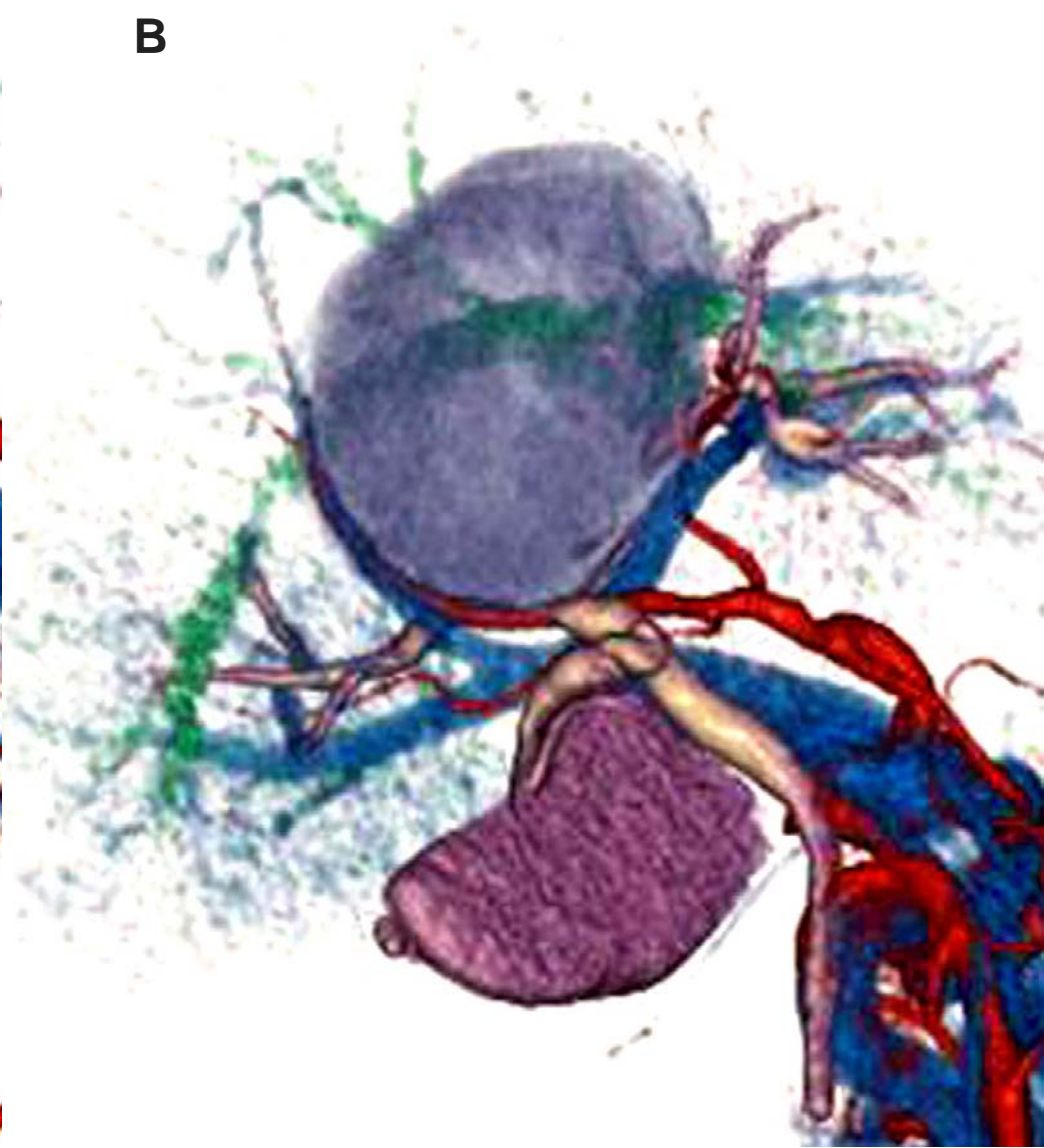
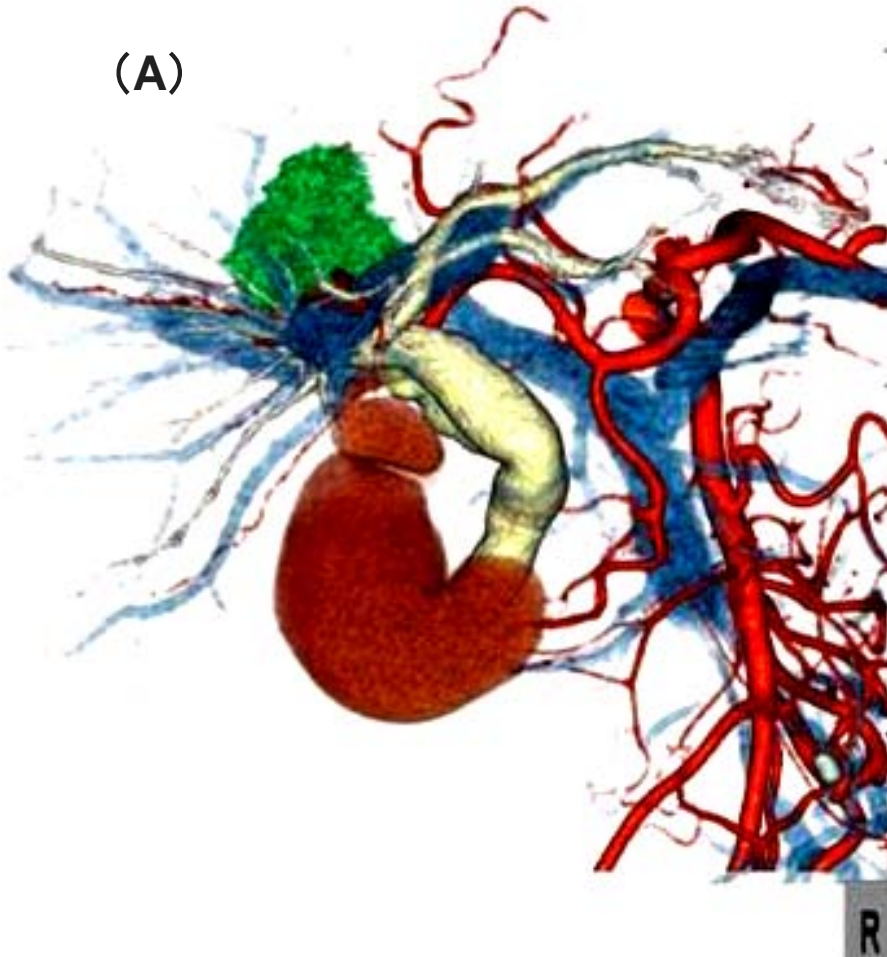


Fig 4

(A)



(B)

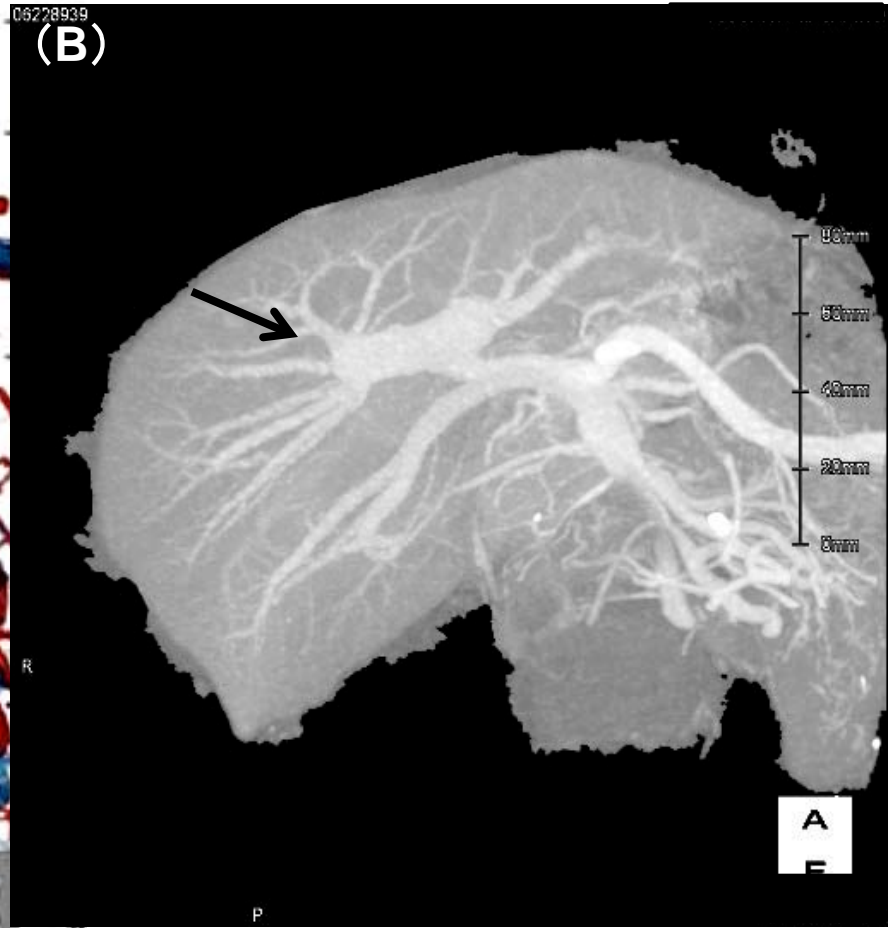


Fig 4

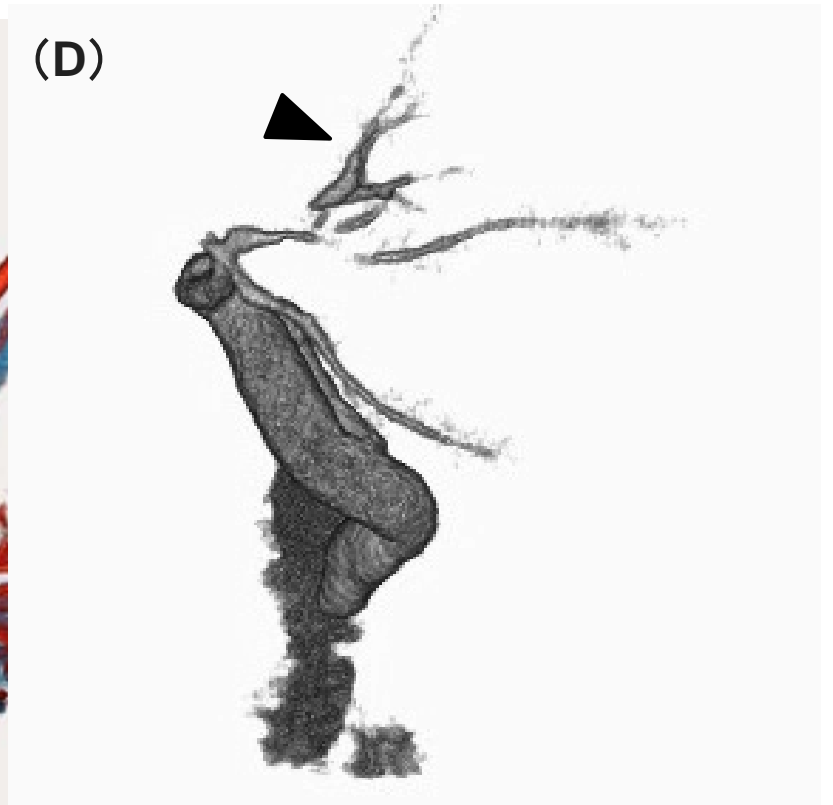
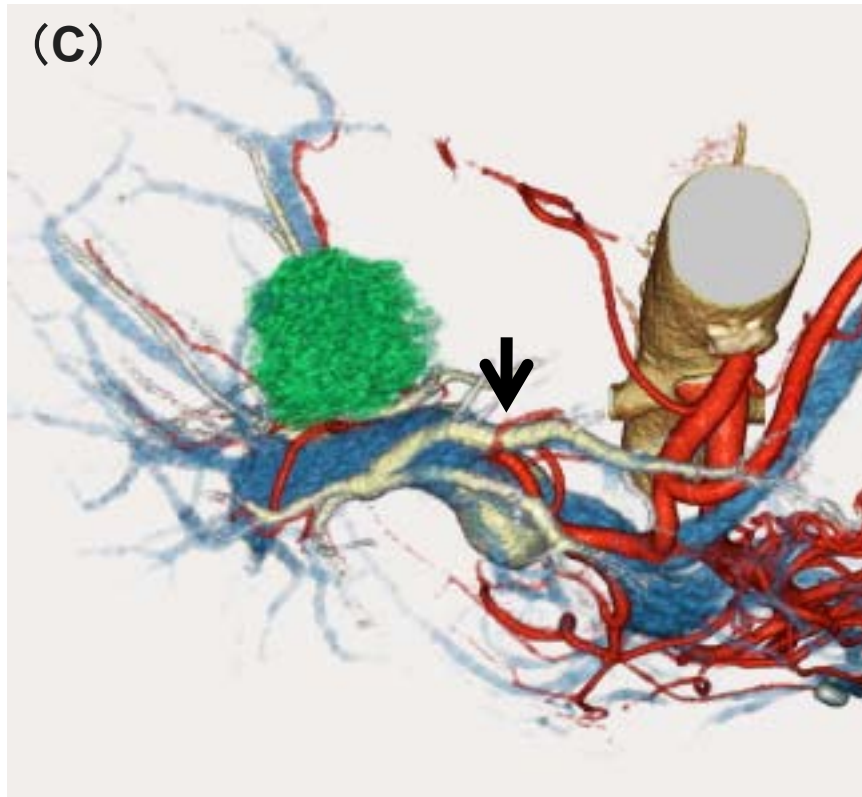
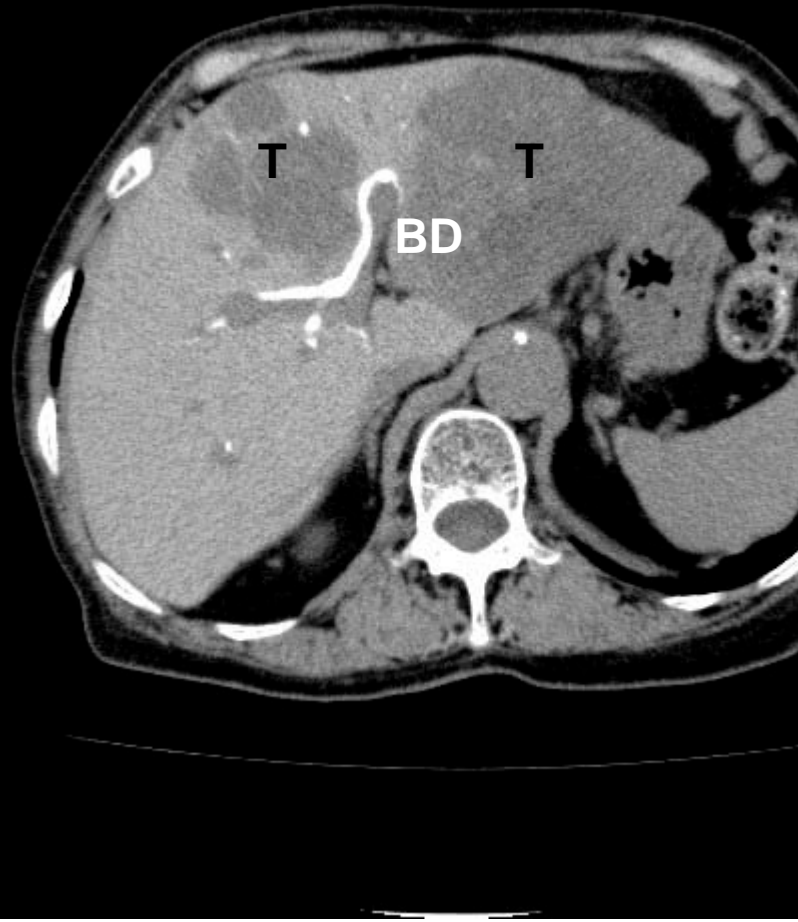


Fig 5



Fig 6

(A)



(B)

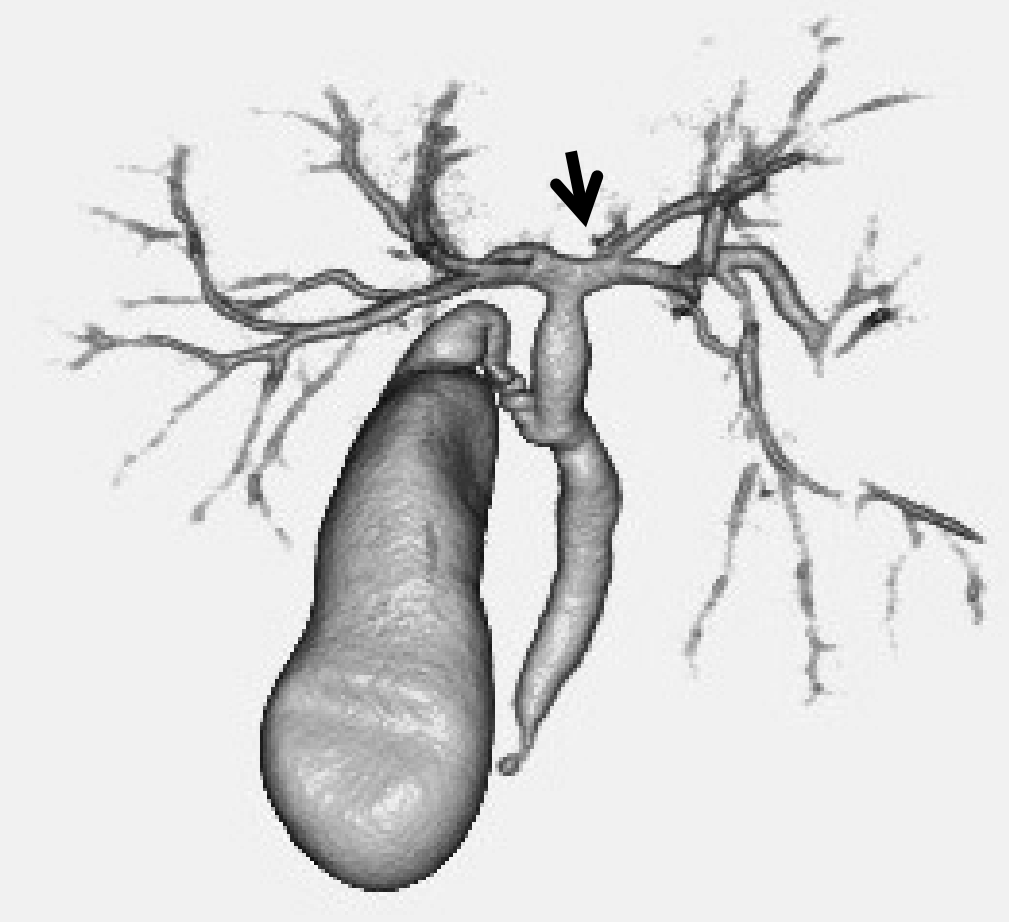


Fig 7

(A)



(B)

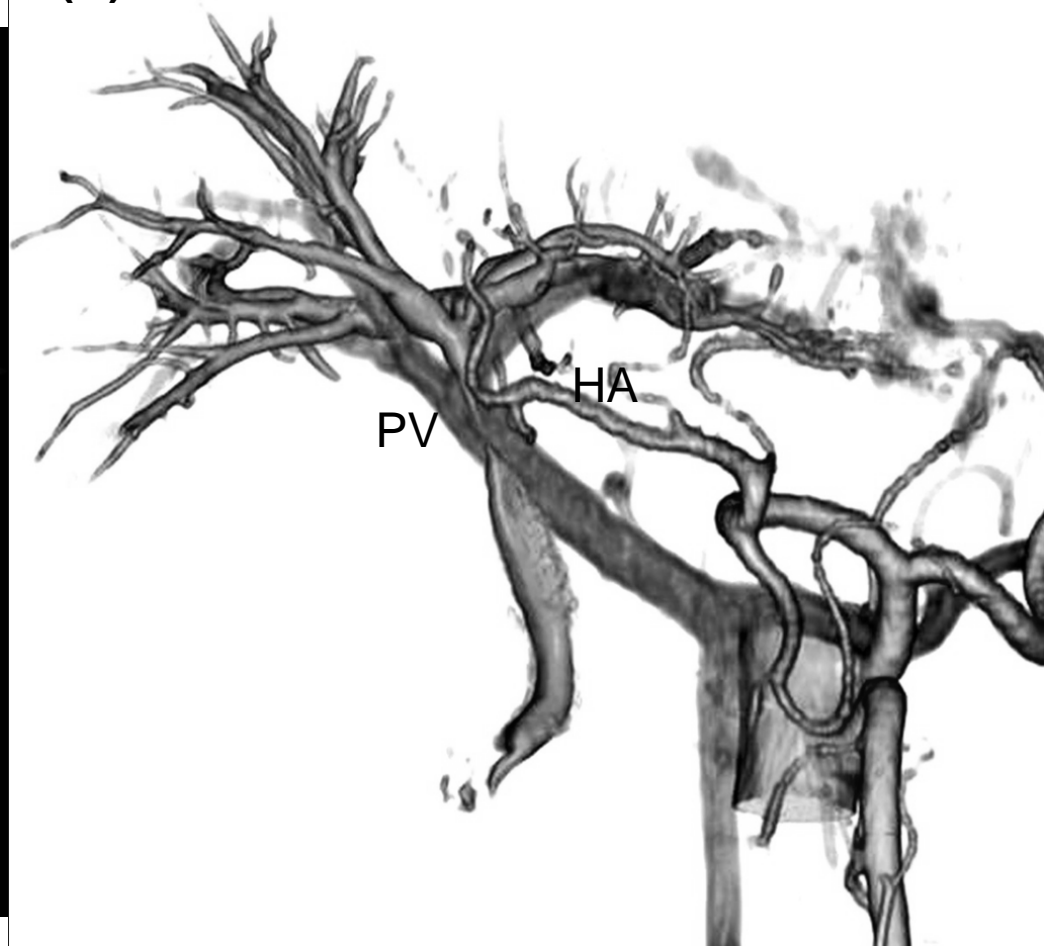


Fig 7

